Proceedings HTR2006:
3rd International Topical Meeting on High Temperature Reactor Technology
October 1-4, 2006, Johannesburg, South Africa

Article number: E00000116

DEVELOPMENT OF 9-12CR MARTENSITIC STEELS FOR FUTURE NUCLEAR SYSTEMS: WELDABILITY STUDIES, MECHANICAL CHARACTERIZATIONS AND SPECIFICATION IMPROVEMENTS

J. L. Séran / CEA/DEN/DMN, Saclay Center, 91191 Gif-sur-Yvette, France

P. Billot / CEA/DEN/DDIN, Saclay Center, 91191 Gif-sur-Yvette, France

G. de Dinechin / CEA/DRT/DTH, Saclay Center, 91191 Gif-sur-Yvette, France

L. Forest / CEA/DRT/DTH, Saclay Center, 91191 Gif-sur-Yvette, France

M. T. Cabrillat / CEA/DEN/DER, Cadarache Center, 13108 St-Paul lez Durance, France

O. Ancelet / CEA/DEN/DM2S, Saclay Center, 91191 Gif-sur-Yvette, France

D. Gaude-Fugarolas / CEA/DEN/DMN, Saclay Center, 91191 Gif-sur-Yvette, France

Y. de Carlan / CEA/DEN/DMN, Saclay Center, 91191 Gif-sur-Yvette, France

G. Merle / AREVA-NP, St-Marcel Technical Center, 71380 Saint-Marcel, France

B. Riou / AREVA-NP Inc, 3315 Old forest road, OF 55, Lynchburg, VA 24501, USA

KEY WORDS:

9-12Cr martensitic steels, future nuclear systems, gas-cooled reactors, pressure vessel, weldability, hot cracking, Varestraint tests, negligible creep, creep-fatigue properties, defect assessment, welded junctions, specification improvement, neural networks, creep prevision.

ABSTRACT

Focusing on the potential use of 9-12Cr martensitic steels for vessel application of the future gas-cooled reactors, this paper deals firstly with a major key issue for this application, namely the weldability of large and thick forged ring that would serve to built the final vessel. This point is identified as critical because the first GTAW (Gas Tungsten Arc Welding) thick weldments have exhibited significant hot cracking located in the weld zone. We have studied the hot cracking sensitivity of this steel with the Varestraint method. This work allows us to give some metallurgical solutions in term of chemical composition of the filler wires used with arc welding processes.

Moreover, aiming at characterizing the mechanical behavior of this steel and of its welded junctions in representative loading situations of a future pressure vessel of a gas-cooled reactor, we present here the more recent results allowing to characterize and predict the creep and creep-fatigue properties of this martensitic steel, as well as the basic data allowing to anticipate the propagation of possible defects in representative conditions of temperature and loading of a reactor vessel.

Starting from the requirement to improve the mechanical resistance of this kind of material for higher temperature applications, the last part of this paper is devoted to the description of our approach for the development of new low activation martensitic steels with improved creep properties. To illustrate the potential of this method, we present here a new family of martensitic steels reinforced by vanadium carbonitrides.

INTRODUCTION

High-Cr ferritic/martensitic steels are promising candidates for nuclear applications because they combine high irradiation resistance, good physical and chemical properties as well as satisfactory mechanical strength at quite high temperature. Among them, 9Cr-1Mo martensitic steels akin to the 91 grade specifications appear as promising prime candidate alloys for the following critical components of the future nuclear power plants [1]: the unirradiated Na circuits of SFR, the weakly irradiated RPV and internals of VHTR/GFR gas reactors and the highly irradiated hexagonal cans of SFR core.

Focusing on the potential use of 9-12Cr martensitic steels for RPV application, this paper deals firstly with a major key issue for this application, namely the weldability of large and

thick (up to 200 mm) forged ring that would serve to built the final 25 m high vessel of the future gas reactors. This point is identified as critical because the first GTAW thick weldments have exhibited significant hot cracking located in the weld zone. Starting from a given geometry of welding, these first experiences had clearly highlighted the fact that the defects were firstly linked to the hot cracking susceptibility of the material used as filler wire. To understand this phenomenon and to propose industrial solutions in view of obtaining satisfactory weldments, we propose to study the hot cracking sensitivity of this steel with the Varestraint simulation method. This approach will allow us to test different commercial heats of filler wire and thus, to derive important relationships between hot cracking tendency and metallurgical variables as initial chemical composition or d-ferrite presence in the weld.

In parallel to this work, studies are in progress in order to check if this material is able to withstand the operating conditions planned for RPV and internals and if it is covered by the existing design codes. In particular, we aim at characterizing the mechanical behavior of this steel and of its welded junctions, in representative loading situations. Regard to a previous paper on this subject [8], in this contribution we will present the more significant results obtained on the following topics: negligible creep characteristics, experimental determination and modeling of cyclic and creep behavior including welded junctions, validation of creep-fatigue design rules, and defect assessment methods.

In order to satisfy Generation IV criteria's about environmental and economic performances of the future nuclear systems, new advanced alloys have to be designed beyond the 91 grade specifications. In this paper, we will present our approach for the development of new low activation martensitic steels with improved creep properties. This methodology is based on neural-network models built from a large database of creep properties combined with thermodynamic calculations. To illustrate the potential of this method, we will present here a new family of martensitic steels reinforced by vanadium carbonitrides.

WELDABILITY STUDIES

The "Submerged Arc Welding" (SAW) and "Gas Tungsten Arc Welding" (GTAW) processes are widely considered as the reference processes to assemble reactor vessel rings. The first welding tests we have carried out with these processes were performed with commercial filler metals. Five different welding filler wires have been tested (table 1).

	C	Mn	P	S	Si	Ni	Cr	Mo	Nb	V	N
1	0,08	1	0,004	0,005	0,18	0,71	9,03	0,9	0,04	0,18	-
2	0,05	0,8	0,002	0,002	0,31	0,7	9,22	1,01	0,02	0,15	0,011
3	0,12	0,6	0,007	0,001	0,27	0,56	8,95	0,95	0,06	0,21	0,05
4	0,08	1,07	0,004	0,003	0,03	0,33	9,06	1,02	0,04	0,24	0.043
5	0,14	0,57	0,006	0,001	0,24	0,71	8,85	0,98	0,05	0,204	0,036

Table 1: Chemical composition of 5 tested filler wires (wt %)

The welding procedure used to realize these joints is the following: before welding both the parts to be welded are heated to 200°C and the temperature is maintained at this temperature between each pass. After welding, the welding joints are characterized to test the requirements of defects absence and to check if the mechanical properties of the weldment belong to the dispersion band required from the standard codification rules.

The first welding tests performed with the GTAW process have highlighted the presence of large cracks in the welded zone. Then, optimized weldments have been obtained, essentially by decreasing welding energy. Although the standard non destructive tests show no large defects, the metallographic observations revealed the presence in the melted zone of micro-cracks (150-200µm) that could be explained via a significant hot cracking tendency known to occur in modified 9Cr-1Mo steels welded by narrow gap welding techniques. Seeing that such defects, even small, cannot be accepted for nuclear vessel applications, a more fundamental study has been launched to identify the origin of these micro-cracks and to suggest possible ways to avoid any defects. In our specific case of welding of thick 9Cr sections (average thickness of the vessel: 180 mm), it has been evidenced that the first parameter playing a major role on hot cracking phenomenon is the nature of the filler material. That is why we present now the preliminary study performed to test the hot cracking sensitivity of 9Cr filler wires used during standard arc welding processes via the Varestraint testing procedure

Varestraint characterization of the hot cracking sensitivity of the modified 9Cr-1Mo steel used as filler wires

The characterization engaged is on the commercial filler materials advised for this steel.

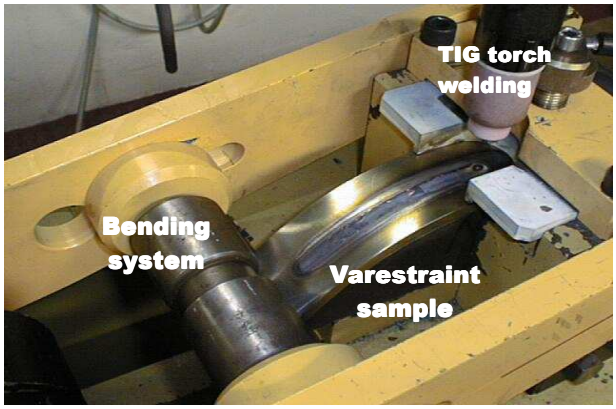

Figure 1: Varestraint device

The principle of the Varestraint method is the following: one end of a rectangular bar (220×49.7×7 mm^3) containing in its center the representative weld metal to be studied is firmly mounted in a fixed position while the opposite is attached to a hydraulic plunger. A GTAW torch produces a melted zone on

the top side of the plate, along its longitudinal centerline, beginning at the unsupported end and moving toward the fixed end. When the welding arc reaches a predetermined location, the plate is bent to conform to the radius of the die block. This induces a defined longitudinal strain on the welded surface of the specimen. Various die blocks with different radii are used to characterize the strain level at which cracking begins. The GTAW welding parameters applied are close to the parameters used to fill the welding joints. For each filler wire, the welding energy is adapted in order to keep constant the geometry of Varestraint melted zone that must be less wide than the width of the filling zone. After this welding simulation procedure, a SEM characterization of mean values of total crack length, number of cracks and maximum crack length is carried out. This method allows us to compare, in the same welding simulation conditions, the hot cracking sensitivity of different materials, particularly the different filler materials described in table 1.

All the cracks induced by the Varestraint test are localized in the weld metal and are perpendicular to the solidification isotherm. The results obtained and the comparisons of the hot cracking sensitivity between each filler wire are given in the figure 2. This representation shows firstly that the strain at which cracking begins is inferior to 1% for all tested alloys and secondly, that we observe very significant differences in the hot cracking sensitivity of these commercial filler alloys.

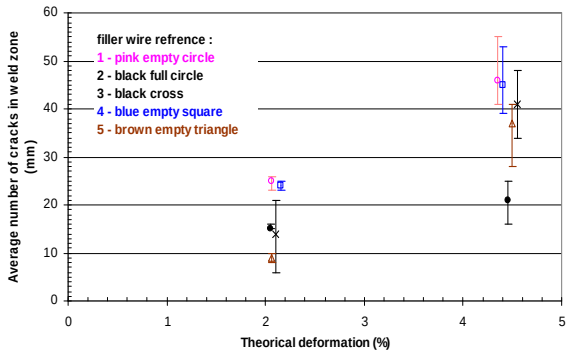

Figure2: Varestraint results, number of crack

In the classification that would be derived from the Varestraint tests, the filler wire 1 is thus much more prone to give hot cracks than the other filler wires.

In addition, SEM and EDS chemical analysis have been carried out around the Varestraint welding cracks of all the materials. Depending mainly on initial sulfur and manganese contents, we generally observe near the cracks end an important increase in the chemical composition of these elements.

Discussion

It is now well established (for a comprehensive synthesis on the subject, see for instance the reference [2]) that, for this kind of steel, a strong relationship exists between the hot cracking sensitivity and the nature and distribution of micro segregations observed during solidification. The elements clearly identified as promoting the cracking via interfacial segregations are mainly sulfur, phosphorus and boron. Among them, sulfur could be particularly detrimental via possible formation of the low melting eutectic MnS. During a welding run, these segregations will depend on the solubility of the different elements in the solidification microstructure. So, to assess the solidification cracking sensitivity, we propose to study the influence of both the chemical composition in S, P and Mn, and the solidification microstructure.

In agreement to this approach, the tested five filler materials will be classified from the following informations:

- Firstly from the results of the Varestraint tests.
- Secondly, one side from the dedicated criteria and diagrams of the literature, as the Lippold diagram [3 - 5] shown figure 3, that are capable of predicting the solidification microstructure and the ferrite content for the mod.9Cr-1Mo steel, and to the other side from the prediction, using the THERMO-CALC software, of the solidification microstructure by measuring the width of the fully ferritic zone in the solidification path (figure 4).

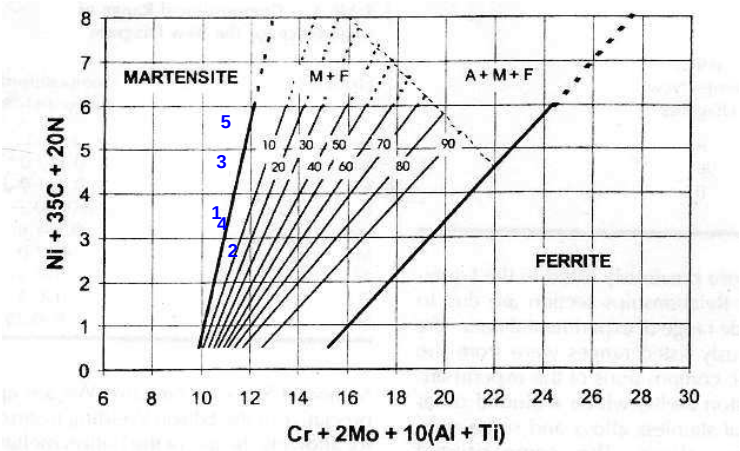

Figure 3: Positioning of tested filler wires on the Lippold diagram (the blue symbols on the diagram indicate each filler wire reference)

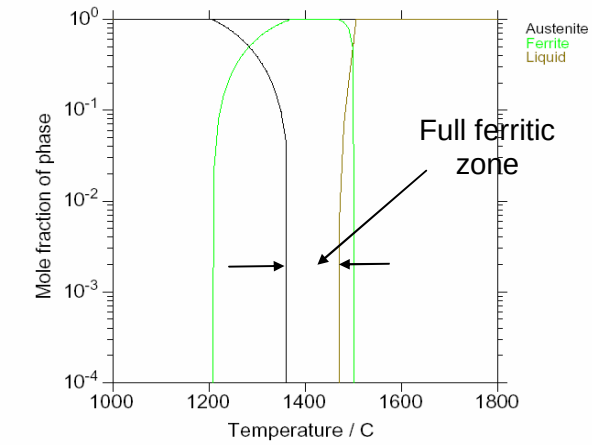

Figure 4: example of the THERMO-CALC analysis of filler wire 2

- Thirdly from the initial content of elements sulfur and phosphorus, known to promote cracking.

- Figure 3 shows that whereas the filler wire 2 is localized in the martensitic-ferritic zone, filler wires 1, 3, 4 and 5 belong to the fully martensitic region. The diagram predicts about 10% of ferrite for filler wire 2. The position of these materials varies mainly with the equivalent nickel. The material 4 is close to the ferritic border.

This first classification in term of tendency to form ferritic phase can be confirmed and quantified via the formula of Kaltenhauser "FF" [3, 6] and equivalent chromium "$Cr_{equivalent}$" [6, 7] criteria or with a THERMO-CALC analysis. The "FF" and "$Cr_{equivalent}$" equations used here are:

$$FF = Cr+6Si+8Ti+4Mo+2Al+4Nb-2Mn-4Ni-40C-40N$$

$$Cr_{equivalent} = Cr+6Si+4Mo+1.5W+11V+5Nb+12Al+8Ti-40C-2Mn-4Ni-2Co-30N-Cu$$

The classification of the 9Cr cracking susceptibility obtained from the literature diagram/criteria, the THERMO-CALC software and the Varestraint tests give strong similarities. From this global analysis of our results, three groups of materials can be distinguished:

- A first group represented by the filler wire 2 exhibiting a low hot cracking sensitivity from the Varestraint tests and being associated both to a strong ferrite tendency and low S and P contents.
- A second group (wires 4 and 1) presenting conversely a high solidification hot cracking sensitivity and being correlated to both high S + P + Mn contents and quite low ferrite tendency.
- Then a last group that, with the filler wires 3 and 5 could illustrate an intermediary behavior in term of cracking sensitivity and S + P + Mn contents.

We propose thus to conclude qualitatively that the hot cracking sensitivity of mod.9Cr-1Mo narrow gap weldments can be reduced by modifying the chemical composition of filler wire in the following ways: to decrease as low as possible the sulfur and phosphorus concentrations, to limit the Mn content at a bottom value allowing to fulfill the other metallurgical requirements and finally, to adjust the other elements in order to develop a definite amount of delta ferrite during solidification.

MECHANICAL CHARACTERIZATIONS

A large R&D program on mod 9Cr-1Mo steel has been undertaken at CEA in order to characterize the behavior of this material and of its welded junctions. A description of this program was presented previously [8], particularly the first results obtained concerning the behavior and damage in fatigue, creep, or creep-fatigue situations, and the defect assessment evaluations. New results obtained in these different fields are summarized below.

Negligible creep domain.

Pressure vessel will operate in the negligible creep domain in order to avoid developing a specific in-service surveillance program. Hence, the determination of this domain is a key point, because it will have consequences on the definition of operating conditions and mainly on nominal temperature levels. The planned life is 60 years, with a loading rate of 80%, which leads to about 4.10^5 hours. The maximum expected fluence for the vessel is estimated to be about 8.10^{18} n/cm^2 (for neutrons with energy > 0.1MeV), which is lower than the end-of-life doses for PWR (Pressure Water Reactors) vessels. It is assumed that such a low fluence level will induce only negligible effect on the mechanical properties. Specific programs are running out in the framework of European collaboration to check this point [9]. In addition, some of the internal structures will operate in the creep range and consequently they have to be designed relatively to creep and creep-fatigue damages.

In RCC-MR design code, a negligible creep domain is defined for austenitic steels. This curve has been established based on a reference stress σ_o and an acceptable creep strain ε_o. In practice the values of σ_o for 316L(N) are not very different from $0.95S_y$ (or $1.05S_m$) in the temperature range of interest. The value considered for ε_o was 0.01%. In RCC-MR issue 2002, no negligible domain is given for mod 9Cr-1Mo steel. It is only indicated that creep is negligible for temperature lower than 375°C, whatever the hold time is. Some studies are in progress in order to check if the methodology developed for austenitic steels can be used for mod 9Cr-1Mo martensitic steel. First evaluations showed that same criteria to derive the curve are not appropriate, mainly due to the fact that firstly, the ratio between allowable stress S_m and yield stress S_y is quite different for both materials (S_m/S_y = 0.9 for 316 at T > 100°C, but S_m/S_y ~ 0.5 for 9Cr) and secondly, that it is necessary to reevaluate the creep strain laws at low temperatures and stress levels [10].

First specific creep tests on mod 9Cr-1Mo steel were performed for these loading conditions. Their analysis showed that RCC-MR creep laws are too conservative for temperatures lower than 500°C, while ASME laws under predict the creep strains. When the temperature increases, RCC-MR predictions are quite good when compared to experimental results, especially for short term tests. On the opposite, ASME has a tendency to under predict short term creep tests, but to give better estimations for long term tests. Complementary tests are necessary in order to define creep strain laws and parameters more reliable in the short and long term time range.

Creep-fatigue behavior

In order to check the validity of creep-fatigue design rules, dedicated tests have been performed on mod.9Cr-1Mo steel. Procedures proposed in ASME and RCC-MR codes are very similar: both approaches evaluate separately fatigue damage and creep damage and then, combine them using a diagram named "creep-fatigue interaction diagram" as shown in the figures 5 and 6. The diagrams proposed in the two codes are quite different: in RCC-MR, the interaction point is (0.3, 0.3) as for austenitic steels, but in ASME it is (0.1, 0.01). So the available domain in creep-fatigue situations will be very different.

If the tests performed were stress controlled during hold time, i. e. the stress value remains constant during the hold time, stress relaxation is not allowed. Such tests are interesting from several points of view: they allow reaching large creep

damage in shorter time than in fatigue-relaxation tests and they avoid to evaluate stress relaxation in creep-fatigue life assessment routines. These tests are described in [11]. Two types of tests were performed:

- In the first series, the elastoplastic strain range value $\Delta\varepsilon_{ep}$ was constant and equal to 0.7% (total strain range), the hold time t_m was imposed when the maximal strain value is reached in tension (T), and the time duration is imposed: tests indicated T_a on figures 3 and 4.
- In the second series, different values of the elastoplastic strain range $\Delta\varepsilon_{ep}$ were tested, the hold time t_m was either in tension (T) (tests indicated Tb on figures 3 and 4) or in compression (C) (tests indicated C on figures 5 and 6), the duration of hold time is not fixed, but the value of the creep strain ε_c during hold time is imposed.

Experimental results are used to test the validity of RCC-MR creep-fatigue design rule. Fatigue damage and creep damage are evaluated for each loading case, and corresponding points are plotted in the interaction diagram (figures 5 and 6). In [11], several evaluations are proposed and discussed. In this paper, we present results obtained:

- In a "best fit analysis", i.e. without margin factors to evaluate damages (mean fatigue curves, mean stress to rupture curve with a stress σ) and using the experimental values of stresses during hold time and of creep strains (figure 5). This analysis allows validating the shape of the diagram, because no margins are included.
- In a "design analysis", i.e. with codified data to evaluate the damages (codified fatigue curve, minimal stress to rupture curve with a stress $\sigma/0.9$), and using the RCC-MR procedure to evaluate the stress value during hold time and the cumulated creep strain (figure 6). This analysis allows checking the validity of the design rule and estimating the margin values. On figures 5 and 6, two diagrams are indicated: interaction diagram itself, and the interaction diagram obtained by introducing a multiplicative factor equal to 20.

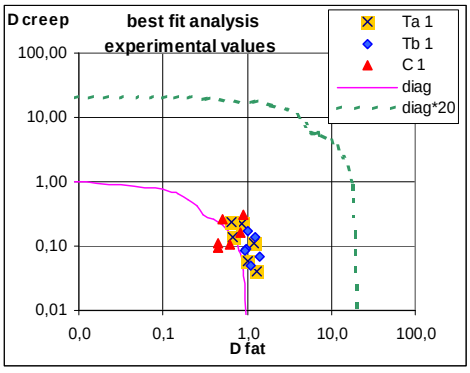

Figure 5: Best fit analysis, using experimental values of stresses and creep strains.

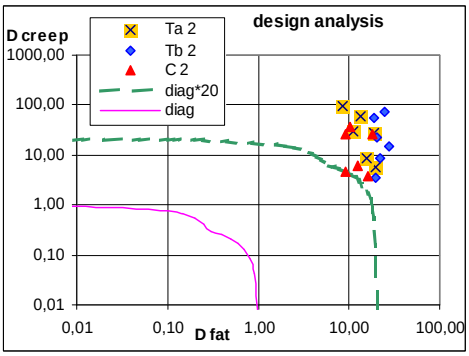

Figure 6: Design analysis with calculated values of stresses and creep strains

We can thus conclude that all the data are correctly located in the interaction diagram. Analyses performed with RCC-MR procedure and RCC-MR codified data allow obtaining a good prediction of these uniaxial experimental results. Estimated margins are quite satisfactory.

In order to complete the test and validation of the creep-fatigue design rules, interpretation of fatigue-relaxation tests and of multiaxial tests or tests on structures with a combination of primary stresses and of cyclic secondary stresses will be performed.

Creep behavior of welded junctions

To predict the creep behavior and the creep life of structures in mod. 9Cr-1Mo steel with welds, physically based models have been developed for the different parts of the weld: BM (Base Metal), HAZ (Heat Affected Zone) and WM (Weld Metal) [8]. The constitutive model developed is a multi-mechanisms model [12]. For the undamaged material, three viscoplastic deformation mechanisms are considered following classical descriptions of creep flow mechanisms: the first one accounts for loading and final rupture stages (quasi plastic flow regime), the second one for viscoplastic creep regime (dislocation climb mechanism) and the third one for diffusional creep regime (grain boundary diffusion mechanism). A coupling between flow and damage is introduced. At each viscoplastic creep mechanism is associated a damage evolution, both nucleation of cavities and their growth by diffusion and by viscoplastic deformation of the matrix are considered. The effect of stress triaxiality is taken into account in nucleation rate.

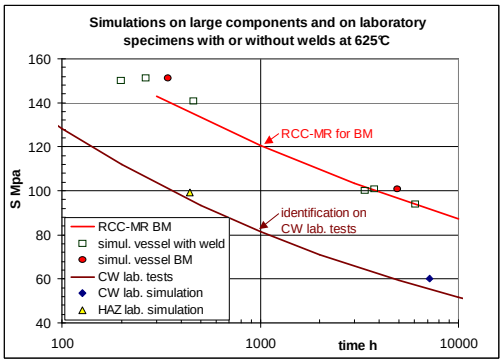

Figure 7: Simulations on large components with or without welds. Comparison with creep life on BM and on CW laboratory samples.

These models are then used to evaluate the life of structures with welds in different loading conditions and to derive the creep joint factors by comparison with similar calculations on structures without welds. First simulations point out that there is a large size effect: for the same stress level, the reduction of life due to the presence of a weld is higher in laboratory samples than in reactor structures (figure 7). This effect can be correlated with the ratio between the width of HAZ and the thickness and diameter of the structure. Small CW (cross-weld) specimens tend to have the same creep life as the HAZ samples, while large components present a creep life close to the BM one. Studies are in progress to characterize more precisely the influence of the different parameters. Tests on large size structures are planned to check this correlation.

Defect assessment

High temperature defect assessment procedures under fatigue, creep and creep-fatigue loadings, have been developed for the fast reactors and have been mainly validated on austenitic stainless steels as 316L(N). Concerning the GCR, complementary studies are conducted in order to validate the existing methods and to get new experimental data on 9%Cr martensitic steels. Moreover, if the geometry and the loadings of a standard CT specimen allow performing a 2D analysis, the case of industrial loadings appears much more complicated, notably because of surface defects which propagate and present shapes that can be considered as half ellipse. Therefore, in the frame of the defect assessment methods validation, the CEA realizes both standard tests on CT specimens to determine the propagation laws and bending tests on large plates under high temperature fatigue, creep or creep-fatigue loadings [8]. These components present an initial semi elliptical surface notch normal to the loading direction and its initiation and propagation are studied. Here, only the determination of the propagation laws for creep loading is presented.

Experimental procedure

The creep tests were carried out on BM and on WM at 550°C on CT specimen (standard side grooved CT 1T). The characteristic dimensions of the CT specimen are: W=50mm, B = 25mm, Bnet = 20mm. They were instrumented to measure both the load line displacement δ(t) and the crack length a(t) by Electric Drop Potential Measurement during the creep test.

*Determination of C**

The load parameter C* is calculated from the load line displacement rate $\frac{\partial \delta_{\exp}}{\partial t} = \dot{\delta}_{\exp}$ which is supposed to split into a part due to the creep behavior noted $\dot{\delta}_C$ and a part due to the structure response related to the crack growth noted $\dot{\delta}_S$: $\dot{\delta}_{\exp} = \dot{\delta}_C + \dot{\delta}_S$ (1)

For each specimen type, C* parameter is calculated using only the part of the load-line displacement due to the creep behavior δ_C which can be calculated with the following equation [13]:

$$\dot{\delta}_C = \dot{\delta}_{\exp} - \frac{\dot{a}B}{F}\left[\frac{2K_I^2}{E^*} + (n+1)J_P^{EPRI}\right] \quad (2).$$

Thus the load parameter C* is formulated as [13]:

$$C^* = \left[2 + 0.522\left(1 - \frac{a}{W}\right)\right]\frac{n_2}{n_2+1}\frac{P\dot{\delta}_C}{B(W-a)} \quad (3).$$

For the 9Cr-1Mo material at 550°C, plastic part of J (noted J_P^{EPRI}) can be neglected.

Determination of the master curve for BM and WM

By merging the results illustrated in figure 8 into a unique da/dt versus C* curve, we can fit a power law $da/dt=AC^{*q}$ for each material:

- $\frac{da}{dt} = 4.8E^{-3}(C^*)^{0.642}$ for the BM;
- $\frac{da}{dt} = 1.85E^{-2}(C^*)^{0.678}$ for the WM.

We can see on this figure the good agreement between the different materials and the important crack growth rate in the WM in comparison to the BM (ratio of 3.8 for a given C*).

test	a_0 (mm)	F (kN)	Test duration (h)	Δa (mm)
GBU4R	27.9	20	1880	2.3
GBU4O	27.6	20	2365	1.9
GBU4X	27.7	22	1244	1.8
GBU4U	27.8	24	460	1.1
GBU4V	27.9	24	358	1.2

Table 2: Creep test conditions at 550°C (BM)
(a_0 is initial crack length; F is the load; Δa is the propagation length of the crack at the end of the test)

test	a_0 (mm)	F (kN)	Test duration (h)	Δa (mm)
2073B1	20.85	24	1488	1.75
2073B4	20.96	27	744	1.48
2073B5	20.5	27	868	1.67
2073B6	21.02	27	912	1.93

Table 3: Creep test conditions at 550°C (WM)

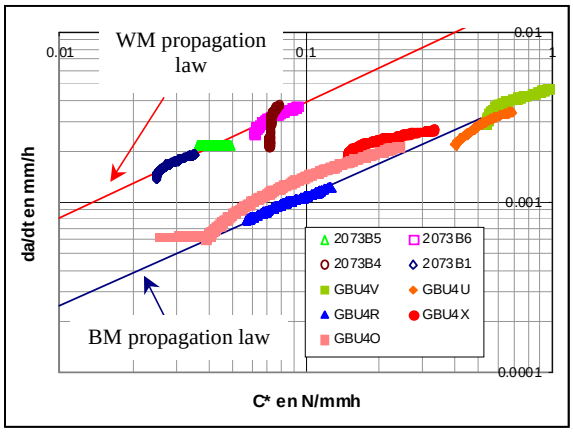

Figure 8: da/dt vs C* curve for BM and WM

SPECIFICATION IMPROVEMENTS

Hitherto, the process to design a new material was mostly heuristic, requiring repeated experimental trial and error, but the accuracy of the present scientific knowledge in thermodynamics and transformation kinetics enables for the successful design of new alloys using minimal empirical feedback. The design process however is still not altogether free of an iterative nature, each stage leading to a more refined definition of the final alloy. The difference with the traditional approach is that most of the process is performed theoretically or computationally, involving the production of only a few essential trial casts to corroborate the suitability of the product material

In the work described here thermodynamic calculations based on the CALPHAD-method [14], and advanced, statistical methods like neural networks [15] are coupled with experimental cast and characterization of a selected sample of alloys are used to develop an optimized set of composition, microstructure and heat treatment to obtain improved creep properties in a new set of alloys for the nuclear power industry [16,17].

A substantial proportion of the alloys for high temperature applications, especially in the power generation industry are based on the Fe8-12Cr system. However, if the alloy needs to work under radiation, some of the additional elements commonly used in the power generation industry and other high temperature applications like Mo, Ni, Nb, Si, Mn, Co and B need to be reduced or even excluded. In that case, these elements are commonly substituted by W, V and Ta. A general range of possible compositions including the elements Fe, Cr, W, V, N, and C but with limited content of Ni, Si, Mn or B was therefore selected for further study. The composition selected allows contemplating the reinforcement of the microstructure with a nanometric distribution of MX-precipitates. VN precipitates, for instance, are stable at higher temperatures than other MX precipitates or $M_{23}C_6$ carbides, and are less prone to coarsening than $M_{23}C_6$ [18]. Calculations of the stability of phases were performed using thermodynamic models based on the CALPHAD method [14].

To determine the effect of small variations of each element on the creep resistance of the alloy, an advanced statistical method was used, a Bayesian-based neural network [15]. Following the analysis using the neural network trained by Cole *et al*. [19, 20], it was obtained that for some elements there was an optimal composition range (represented as a maximum in the predicted creep rupture strength at 10,000 hours). This is the case for Cr and W, elements for which the optimal content were around 9.5wt.% (Figure 9) and 2wt.% (Figure 10) respectively. In the case of chromium this value lies in the lower end of the range of compositions traditionally used for high temperature applications, and therefore it will be needed to pay special attention to aspects like corrosion resistance of the alloy. Tungsten is usually added to produce solid solution strengthening of the matrix, but it is also a strong α-stabilizing element. Carbon also produces a strong solid strengthening effect, and according to the neural network predictions the creep rupture strength of the alloy increases monotonically with the carbon content of the matrix (Figure 11).

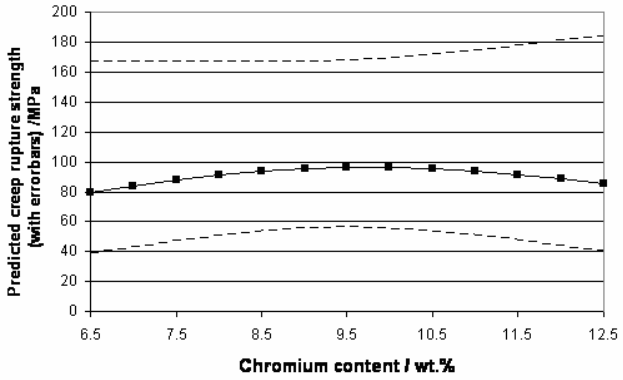

Figure 9: Creep rupture strength as a function of chromium content predicted using a neural network.

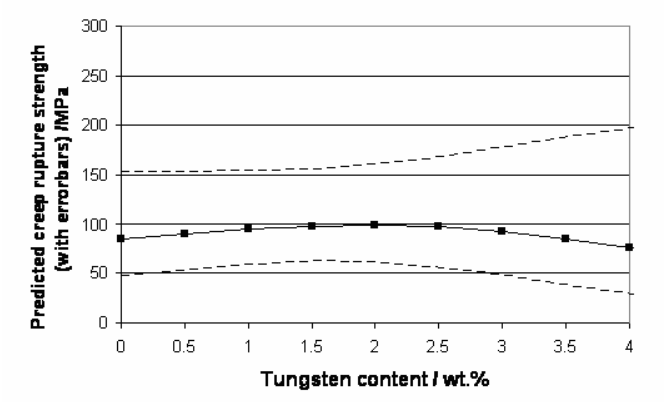

Figure 10: Creep rupture strength as a function of tungsten content predicted using a neural network.

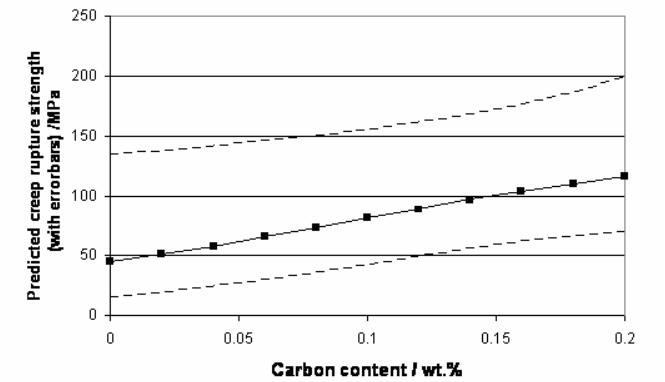

Figure11: Creep rupture strength as a function of carbon content predicted using a neural network.

Carbon is also a strong γ-stabilizing element, which helps to compensate for the increase in α-stabilizing elements like W or V. However, this trend needs to be taken cautiously, as not all carbon stays in solid solution but it tends to precipitate as $M_{23}C_6$. $M_{23}C_6$ precipitates have rapid coarsening kinetics and therefore produce little improvement in the mechanical properties, and on the other hand steal Cr from the matrix of the alloy, reducing its oxidation resistance. Better results are expected from a fine distribution of MX precipitates (*i.e.* VN), which on one hand coarsen more slowly, allowing for a potential improvement in creep resistance and toughness, and on the other hand are stable at higher temperatures. VN precipitates are able to play that strengthening role, and so it would seem at first to be interesting to increase the content in both V and N. Indeed, the creep rupture strength increases with the vanadium content (Figure 12) but this element is at the same time a strong α-stabilizing element, and an excess of it would prevent the complete austenitization of the alloy. On the other hand the predictions of the neural network suggest that the optimal nitrogen content lies around 0.07wt.%, as shown in Figure 13.

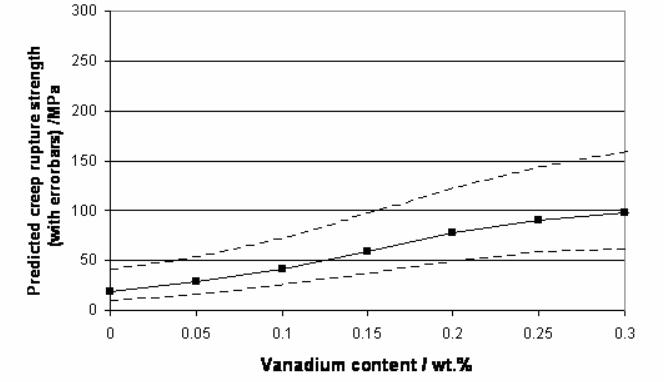

Figure 12: Creep rupture strength as a function of vanadium content predicted using a neural network.

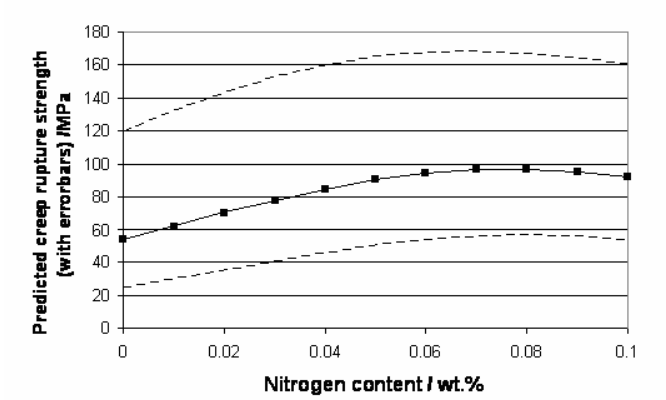

Figure 13: Creep rupture strength as a function of nitrogen content predicted using a neural network.

Finally, Figure 14 shows that the predicted creep rupture strength increases with boron content. Even small additions of boron have important influence on creep behavior of Cr-steels, as it diffuses to the surfaces of $M_{23}C_6$ precipitates, specially to those close to previous austenitic grain boundaries and slows down their coarsening [21]. Boron is an element that, on its natural form is deleterious in alloys exposed to radiation. However, if only small amounts are needed, isotope B^{11} could be used, which does not form helium under radiation like B^{10} and still be able to benefit from the effect of boron.

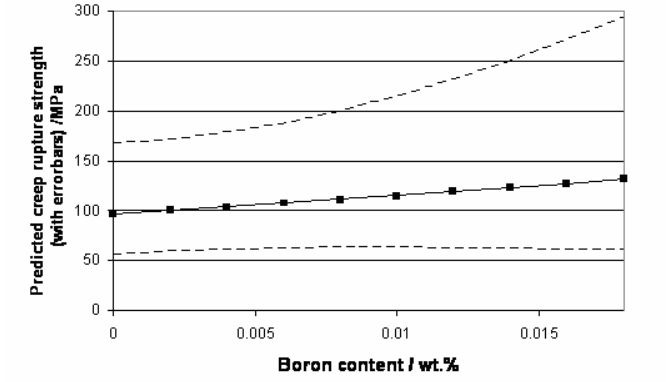

Figure 14: Creep rupture strength as a function of boron content predicted using a neural network.

To conclude, after examining the related literature and analyzing the possible compositions with the help of advanced statistical methods, an alloy composition optimized to maximize the creep rupture strength and presenting good oxidation properties was chosen. The proposed composition is (with all compositions expressed as wt. %) Fe 9.5Cr 0.14C 2.5W 0.35V with up to 0.07N and with the possibility of small (less than 0.1wt. %) additions of B^{11} .

The next step in the design of a new alloy is to develop the right thermo-mechanical treatment to obtain the desired microstructure, and in particular the optimal distribution of precipitates. To that end, a software *suite* combining the CALPHAD method of thermodynamic stability calculations with precipitation kinetics models becomes essential [22]. Using a thermodynamic and kinetics software like MatCalc

enables us to predict the effect of various microstructure parameters like, grain and sub-grain size, deformation level and thermo-mechanical treatment parameters on the precipitation kinetics and final size distribution of the various species of precipitates [16].

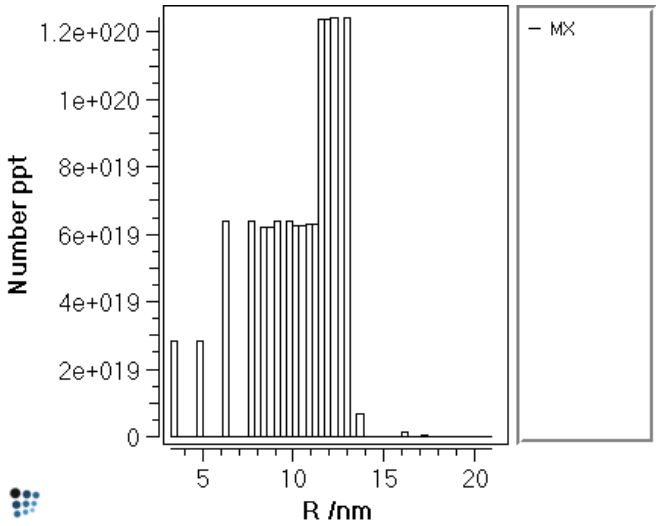

Figure 15: MX precipitate size distribution.

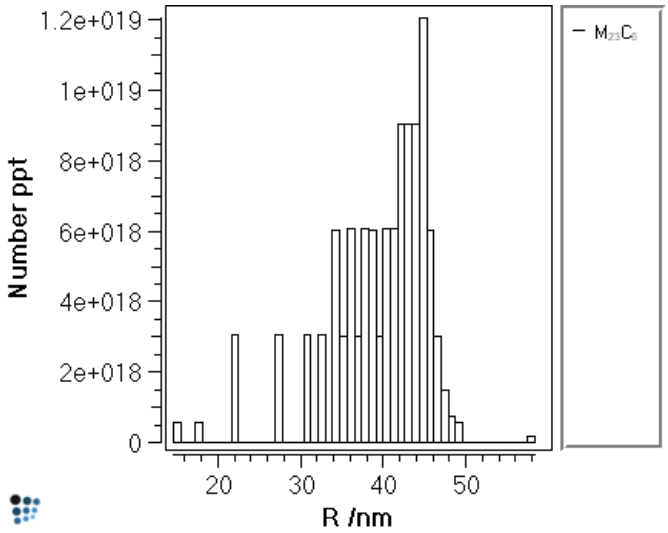

Figure 16: M23C6 precipitate size distribution.

As an example, the alloy described above has been simulated to follow a heat treatment consistent in austenitization at 1175°C; quench in oil and finally temper at 750°C for 10h. Figure 15 shows an estimate of the distribution of MX precipitates (in this case vanadium carbo-nitrides), and Figure 16 the distribution of $M_{23}C_6$ precipitates after the treatment according to the simulation. More details of the calculation have been published elsewhere [16].

This work intends to show the valuable potential of advanced modeling into the design and development of new alloys for all sorts of critical applications.

CONCLUSION

In this article we have presented the more recent works launched at CEA to qualify the 9Cr-12Cr as possible generic structural material for nuclear components.

Regarding the vessel application, the first critical point is the assembly of the large forged rings to form the vessel: to improve the weldability of the 9Cr that is prone to exhibit hot cracking when welded in large thickness and thus, to prevent the weldments to contain defects we propose some requirement in term of chemical composition of the filler wires used with the arc welding processes.

To verify that this material is capable to withstand the operating conditions planned for RPV and internals and if it is covered by the existing design codes we have launched a large program aiming at characterizing its mechanical behavior in representative operating conditions. From this program we show that analyses of creep and fatigue damages performed with RCC-MR procedure and RCC-MR codified data allow obtaining a good prediction of the experimental uniaxial results. Moreover, the estimated margins are quite satisfactory. Complementary analyses will be performed to extend the validation domain. Then, the models built to evaluate the creep life of the welded junctions are described and compared to experimental data. Finally we present the creep crack propagation laws for the base metal and the weld metal.

Because we need, on these steels, higher creep resistance in order to satisfy Generation IV criteria's about environmental and economic performances of the future nuclear systems, the third part of the program concerns the development of new advanced alloys beyond the 91 grade specifications. Using Neural-network models based on a large database of creep properties combined with thermodynamic calculations we give the main rules to define the chemical composition of an advanced martensitic steels reinforced by vanadium carbonitrides.

REFERENCES

[1] P. Billot, J. L. Séran, M. T. Cabrillat, H. Burlet, A. Terlain, J. P. Bonal, "CEA R & D program on structural materials for the Very High Temperature Reactor (VHTR)", paper presented at the GLOBAL 2003 Conference, November 17-20, 2003, New Orleans, Louisiana, USA.

[2] R. L. Klueh and D. R. Harries, "High-Chromium Ferritic and Martensitic Steels for Nuclear Applications", Chapter 7, ASTM Publication, 2001.

[3] « Delta formation in 9-12% Chromium Steel Weldments », E.Ayala, M.A. Roman, J. Vega, X. Gomez, T. Gomez-Acebo and J. Echeberria, Advanced heat resistant steel for power generation, 1999, pages 633-643

[4] « A preliminary ferritic-martensitic stainless steel constitution diagram », M.C Balmforth, J.C. Lippold, Welding journal, Janvier 1998, pages. 2s-6s

[5] « A new ferritic-martensitic stainless steel constitution diagram », M.C. Balmforth, J.C. Lippold, Welding journal, Décembre 2000, pages 339s-345s

[6] « The Effect of composition on microstructural development and mechanical properties of modified 9% Cr

1%Mo weld metals », A.M. Barnes, Microstructural stability of creep resistant alloys for high temperature plant application (conference), Sheffield, UK, Mars1997

[7] « Influence of Co, Cu and W on microstructure of 9%Cr steel weld metals », R.G. Faulkner, J.A. Williams, E. Gonzalez Sanchez, A.W. Marshall, 2003

[8] Cabrillat M.T., Reytier M., Sauzay M., Mottot M., Gaffard V., Seran J.L., Billot P. and Riou B., "Studies on mechanical behavior of mod 9Cr-1Mo steel, CEA R&D program", 2nd International Topical Meeting on High Temperature Reactor Technology, Beijing, China, September 2004.

[9] Buckthorpe D., "Results from EU 5th framework HTR projects HTR-M & M1", 2nd International Topical Meeting on High Temperature Reactor Technology, Beijing, China, September 2004.

[10] Riou B., Escaravage C., Swindeman B., Ren W., Cabrillat M.T. and Allais L., "Negligible creep conditions for mod 9Cr-1Mo steel", ASME ICPVT11, Vancouver, July 2006.

[11] Cabrillat M.T., Allais L., Mottot M., Riou B and Escaravage C., "Creep fatigue behavior and damage assessment for mod 9Cr-1Mo steel", ASME ICPVT11, Vancouver, July 2006.

[12] Gaffard V., Besson J. and Gourgues F., "Creep failure Model of a 9Cr-1MoNb steel integrating multiple deformation and damage mechanisms", ECF15, Stockholm, 2004.

[13] ASTM E 1457-98, Standard test method for measurement of creep crack growth rates in metals,

[14] Saunders, N. and Miodownik, A.P. 1998, CALPHAD, calculation of phase diagrams, a comprehensive guide. Pergamon Press, Oxford, UK.

[15] MacKay, D.J.C. 1997, "Bayesian non-linear modelling with neural networks", Mathematical modelling of weld phenomena 3. The Institute of Materials. London, UK.

[16] Gaude-Fugarolas, D., Yardley, V., Lardon, J-M., Montagnon, J., De Carlan, Y. 2006 "Advanced alloy design tools applied to the development of vanadium nitride strengthened high-temperature steels", Proc. 8th Liege Conference Materials for Advanced Power Engineering. Liege, Belgium.

[17] Yardley, V. A. and De Carlan, Y., 2006," Design criteria for high-temperature steels strengthened with vanadium nitride", Journal of Phase Equilibria and Diffusion, Vol.27, pp.102-112

[18] Bhadeshia, H.K.D.H., 2000, "Design of heat resistant alloys for the energy industries", Proc. of 5th International Charles Parsons Turbine Conference, Cambridge, UK

[19] Cole, D., Martin-Moran, C., Sheard, A.G., Bhadeshia, H.K.D.H. MacKay, D.J.C., 2000, "Modelling creep rupture strength of ferritic steel welds", Science and Technology of Welding and Joining, Vol.5, pp.81-89

[20] De Carlan, Y., Murugananth, M., Sourmail, T., Bhadeshia, H.K.D.H., 2004, "Design of new Fe-9CrWV reduced-activation martensitic steels for creep properties at 650°C", Journal of Nuclear Materials, Vol.329-333, pp.238-242

[21] Abe, F., Horiuchi, T., Taneike, M., Sawada, K., 2004, "Stabilisation of martensitic microstructure in advanced 9Cr steel during creep at high temperature", Materials Science and Engineering A, Vol.A378, pp.299-303

[22] Svoboda, J., Fischer, F. D.,Fratzl, P.,Kozeschnik, E., 2004 "Modelling of kinetics in multi-component multi-phase systems with spherical precipitates I: Theory", Materials Science and Engineering A, Vol.A385, pp.166-174

